Supporting Information

for

Visualized Metabolic Disorder and its Chemical Inducer in Wild Crucian Carp from Taihu Lake, China

Shixiong Gao[1#], Hang Liu[1#], Hong Chang[2], Zhaobin Zhang[1], Jianying Hu[1], Shu Tao[1], Yi Wan*[1]

[1]*Laboratory for Earth Surface Processes*, College of Urban and Environmental Sciences, Peking University, Beijing 100871, China
[2]*Beijing Key Lab for Source Control Technology of Water Pollution*, College of Environmental Sciences & Engineering, Beijing Forestry University, Beijing 100083, China

[#]Contributed equally

[*]Corresponding author: Yi WAN,

College of Urban and Environmental Sciences,

Peking University, Beijing 100871, China,

TEL & FAX: 86-10-62765520,

Email: wany@urban.pku.edu.cn.

Texts

Tables

Figures

Figures S4-S13. The chromatograms and fragmentation spectrums of phospholipids (PLs), polypeptides (PPs), fatty acyls (FAs), sterol lipids (SLs), glycerides (GLs), prostaglandins, vitamins, saccharides, amides, and red pigments identified in blood samples of wild crucian carp from Taihu Lake.

Figure S14. Profile variations of the intrinsic metabolites in carp exposed to the identified exogenous pollutants (*in vivo*).

Chemicals and Reagents.

The following isotopically labeled standards used in this study were purchased from Avanti Polar Lipids (Alabaster, USA) and had purities of ≥98%: 16:0 D31 ceramide (CER), 16:0-D31 sphingomyelin (SM), 16:0 D31-18:1 phosphatidylglycerol (PG), 16:0 D31-18:1 phosphatidylinositol (PI), 16:0 D31-18:1 phosphatidylethanolamine (PE), 16:0 D31-18:1 phosphatidylserine (PS), 16:0 D31-18:1 phosphatidylcholine (PC) and D7 sphingosine (SPH). Progesterone-d9 and 17β-estradiol-d4-sulfate of >98% purity were purchased from CDN Isotopes (Quebec, Canada). Perfluorooctane sulfonate (n-PFOS, >99%), 3m-perfluorooctane sulfonate (3m-PFOS, >99%), 6m-perfluorooctane sulfonate (6m-PFOS, >99%), dodecylbenzene sulfonic acid hard-type mixture (SDBS, >95%), di-isobutyl phthalate (DiBP, >99%), 4-n-nonylphenol (NP, >99%), and perfluoroundecanoic acid (PFUnDA, >99%) and bisphenol A (BPA, >99%) were obtained from ANPEL Laboratory Technologies Inc (Shanghai, China). Pesticide residue-grade methyl *tert*-butyl ether (MTBE), methanol (MeOH), chloroform, acetone, isopropanol, and acetonitrile were obtained from Fisher (New Jersey). Formic acid (HPLC grade) was obtained from Dikma Technology INC (Lake Forest, CA). Ammonium hydroxide (28% NH_3) was obtained from Alfa Aesar (Ward Hill, MA). Saline solution (0.9%) was obtained from Shandong Hualu Pharmaceutical Co. Ltd. (Shandong, China). Deionized water was obtained from a Millipore Milli-Q Synthesis water purification system (Bedford, MA).

Sample Preparation.

The polar and nonpolar factions were separately extracted from the whole blood samples through different extraction processes. Samples were firstly thawed on ice, and 50 μL aliquots

were taken and deproteinized with 1.5 mL of iced methanol for extraction of polar components (Fraction 1, F1). After ultrasound-assisted extraction in an iced-water bath for 15 mins, all samples were centrifuged (4 °C, 7500 rpm) for 10 mins. The methanol supernatants of the resulting centrifuged samples were lyophilized to dryness and stored at -80 °C before analysis. Another 50-μL aliquots of whole blood samples were transferred into 4-mL vials for the extraction of nonpolar components and treated with 400 μL of iced MeOH and 100 μL of water to precipitate proteins (Fraction 2, F2). The mixture was vortexed for 2 min and treated with 1.4 mL of MTBE. The resulting mixtures were then ultrasonicated at 4 °C for 15 min, and treated with 500 μL of water to induce separation of the organic layer. The samples were then centrifuged for 10 min (4 °C, 7500 rpm) and the entire organic phases (MTBE) were transferred into new vials. The MTBE extracts were then lyophilized to dryness and stored at −80 °C before analysis.

The residues of F1 and F2 extracts were re-dissolved in 200 μL of methanol/water (1:1, v:v) (F1 samples) and chloroform/methanol/water (1:2:0.8, v:v:v) (F2 samples), respectively. Then the samples passed through a hydrophobic PTFE filter (13 mm, 0.22 μm), and analyzed with an ultrahigh-pressure liquid chromatography (UPLC) system coupled to a quadrupole time-of-flight mass spectrometer (QTOF-MS). Quality control (QC) samples for both polar and nonpolar fractions (F1 and F2) were prepared by pooling 10 μL of each blood sample and pretreating these pooled samples as for the field samples. To resulting QC samples were evenly distributed throughout the analytical sequence to verify the stability and accuracy of the analytical method.

Instrumental Analysis.

Nontargeted acquisitions of the full mass spectra of the components in both F1 and F2 fractions of the blood samples were obtained using a Waters ACQUITY UPLC coupled to a Xevo QTOF-MS (G2, Waters) operating in both the positive (ESI^+) and negative (ESI^-) electrospray ionization modes. An ACQUITY UPLC BEH C18 column (2.1 × 100 mm; 1.7-μm particle size) was used for chromatographic separation of the F1 fraction: solvent A was 0.1% formic acid in ultrapure water (containing 5% acetonitrile), solvent B was acetonitrile, and the flow rate was 0.3 mL min^{-1}. In the positive mode, the gradient was 5% B at 0–0.5 min and was ramped to 22% B at 0.5–3 min, to 50% at 3–6 min and held for 2mins, and finally to 100% B at 8–10 min, before being equilibrated to initial conditions at 10–11 min and held for 2 min before injection of the next sample. In the negative mode, the initial conditions of 5% B were held for 0.5 min and then ramped to 22% B at 0.5–4 min, to 75% B at 4–5 min, finally to 100% B at 5–7 min, before equilibration to initial conditions at 7–9 min and held for 2 min before the injection of the next sample. The column was maintained at 30°C, and the injection volume was 3 μL. For screening the molecules in the F1 fraction, mass spectrometry was performed in continuum mode in the m/z range of 50–1200 for both the ESI^+ and ESI^- modes to acquire high-accuracy MS^E data of the precursor ions. The fragmented mass range was also 50–1200 m/z. In low-energy mode, data were collected at a constant collision energy of 4 V, and in elevated energy mode, the collision energy was ramped from 15 V to 50 V. The other optimized parameters were as follows: multiplier voltage, 4 V; source temperature, 100°C; desolvation gas temperature, 250°C; cone gas flow, 50 L/h; desolvation gas flow, 600 L/h; source capillary voltage, 2.7 kV (ESI+) or 2.5 kV (ESI−); sampling cone voltage, 40 V (ESI+) or 45 V (ESI−). For screening the molecules in the F2 fraction, the parameters of MS

were identical to those used for the F1 fraction for both the ESI+ and ESI− modes except for some optimized parameters: multiplier voltage, 4 V; source temperature, 100°C; desolvation gas temperature, 400°C; cone gas flow, 50 L/h; desolvation gas flow, 600 L/h; source capillary voltage, 3 kV (ESI+) or 2 kV (ESI−); sampling cone voltage, 40 V (ESI+) or 45 V (ESI−).

An ACQUITY UPLC BEH C8 column (2.1 × 100 mm; 1.7 μm particle size) was used for chromatographic separation of the F2 fraction: solvent A was 0.1% ammonium in ultrapure water, solvent B was 15% isopropanol in methanol, and the flow rate was 0.2 mL min^{-1}. In the positive mode, the gradient was 30% B at 0–0.5 min and was then ramped to 50% B at 0.5–2 min, to 70% B at 2–3 min, to 90% B at 3–4.5 min, and finally to 100% B at 4.5–5 min and then held for 3 min, before being equilibrated to the initial conditions at 8–9 min and held thus for 3 min before injection of the next sample. In the negative mode, the initial conditions of 30% B were held for 0.5 min, and the gradient was then ramped to 50% B at 0.5–2 min, to 95% B at 2–3 min, and finally to 100% B at 3–5 min and then held for 3 min, before equilibration to the initial conditions at 8-9 min and being held for 3 min before injection of the next sample. The column was maintained at 40 °C, and the injection volume was 3 μL. The mass spectrometry parameters in the continuum mode were identical to those used for the F1 fraction for both the ESI^+ and ESI^- modes to acquire high-accuracy MS^E data for all precursor ions, although some variation was seen in the other optimized parameters, as follows: multiplier voltage, 4 V; source temperature, 100°C; desolvation gas temperature, 400°C; cone gas flow, 50 L/h; desolvation gas flow, 600 L/h; source capillary voltage, 3 kV (ESI^+) or 2 kV (ESI^-); sampling cone voltage, 40 V (ESI^+) or 45 V (ESI^-).

High-Throughput Identifications of Mass Signals.

For runs obtained in the ESI^+ and ESI^- modes for both F1 and F2 fractions, a suitable sample was auto-selected as the reference sample for peak alignment to compensate for the between-run variation in the chromatography results.[1] According to the typical ionization behavior of intrinsic metabolites and exogeneous chemicals, $[M+H]^+$, $[M+K]^+$, $[M+Na]^+$, $[M+NH_4]^+$, and $[M+H-H_2O]^+$ and $[M-H]^-$, $[M-H_2O-H]^-$, $[M+FA-H]^-$, and $[M+CH_3COO]^-$ were selected as the adduct ion forms in the ESI^+ and ESI^- modes, respectively.[2] During the peak-picking procedure, the sensitivity was set to 3 and the minimum chromatographic peak width was set to 0.1 m to acquire the maximum detectable ion signals while excluding noise. For peak identification of both intrinsic metabolites and exogeneous pollutants, mass signals with ion mass errors <10 ppm and isotope similarity >50% were identified by searching against the following online mass databases: the Human Metabolome Database (HMDB), the Kyoto Encyclopedia of Genes and Genomes (KEGG), Lipid Maps, and Mass Bank. The remaining unmatched mass signals were then identified by searching against the PubChem and PubMed databases with the same conditions. For the molecules that were identified in both ESI+ and ESI- modes or both F1 and F2 fractions, the peaks with higher abundances and matching rates were listed in the final identification results. All duplicate identified results were manually screened.

Validation of Identified Intrinsic Metabolites and Exogenous Chemicals.

All intrinsic metabolites in blood samples of the wild crucian carp were identified by both MS and corresponding MS/MS information recorded in the database. The results belonged to the second level of identifications, as described by the Metabolomic Standards Initiative

(MSI).[3] The representative metabolites were further validated by analyzing the fragmentation patterns generated by the collision-induced dissociations in the MS^E analysis. The recoveries of the metabolites were confirmed by a spiking experiment. Because blood contains relatively high concentrations of intrinsic metabolites such as phospholipids, glycerides, and cholesterols, the spiking experiment was conducted with deuterated standards.[4] The recoveries of the deuterated standards in F1 factions (progesterone-d9 and 17β-estradiol-d4-sulfate) and F2 factions (16:0 D31 CER, 16:0-D31 SM, 16:0 D31-18:1 PG, 16:0 D31-18:1 PI, 16:0 D31-18:1 PE, 16:0 D31-18:1 PS, 16:0 D31-18:1 PC and D7 SPH) were in the range of 88.6% to 93.6% and 63.6% to112.4%, respectively.

The chemical structures of suspect pollutants were identified by MS/MS analysis with the same instrumental parameters listed above, except that the MS^2 collision energies comprised three channels set to 5–15 eV, 15–30 eV and 30–45 eV, respectively. The structures of the identified chemicals were confirmed by their distinctive MS/MS spectra and molecular ions, and the identifications were belonged to the second level. For chemicals with significantly regional differences and potentials to induce metabolic disorders, the commercial standards were purchased to realize the first levels identification of the compounds, and further used for exposure experiments with wild crucian carp.

Network Correlation Analysis.

Peak intensities of detected signals was firstly normalized, and the missing values were filled with zeros according to the commonly used methods.[5] The interactions between every two signals were evaluated by correlation analysis with the Pearson correlation coefficients (R) determined by MATLAB (MathWorks, MA). The coupled compounds with close relationship

were further selected for network correlation analysis based on that an R value was greater than 0.7. In the network, each signal was represented as a node, and the corresponding pairwise connections were represented as links between two pairing compounds (edges). The network was automatically modularized and processed with a force-directed layout algorithm (OpenOrd) to distinguish the core clusters of the compounds detected in the blood from wild crucian carp. The marginal isolated nodes were removed as outliers, and the final correlation network was obtained using the Force Atlas layout algorithm for distinct clustering and manual optimization. All parameters of the applied algorithms were listed in Table S3. To facilitate the discrimination of the intrinsic metabolites and their interactions in the pathways, the nodes that belonged to several representative metabolic classes that were present in higher amounts were filled with different colors in the network, and their sizes were set to a value from 15–50 in proportion to their extent of nodal connectivity. Network correlation analysis of the screened compounds in the blood samples was achieved by processing the coupled interactions in Gephi 0.9.1 (Gephi Consortium, France). A video that shows the establishment of the network is provided in the Supporting Information (Video S1).

In the *in vivo* exposure tests, the identified intrinsic metabolites were matched with the network established for the metabolites found in the blood of the wild crucian carp in Taihu Lake. The abundance ratios of the matched intrinsic metabolites (treated groups/control group) were imported into the network to evaluate the toxic effects of exposed chemicals on the crucian carp. The alterations of the intrinsic metabolite profiles of the exposed carp were examined to explore the pollutants that were responsible for inducing the metabolic disorders in wild crucian carp.

Multivariate Statistical Analysis.

In all analyses, normalized intensities were used for all identified molecules. An independent-sample *t*-test was used to select the intrinsic metabolites and pollutants with levels that were significantly different in wild samples from different bays in Taihu Lake. Analysis of variance was used to compare the exposure and control groups in the *in vivo* exposure tests. The statistical analysis was performed using SPSS (v24.0; IBM Corp.), and *p* values of less than 0.05 were considered to indicate statistical significance.

Table S1. Concentrations of the chemicals injected to the crucian carp in the exposure tests.

Chemical / Group	PFOS	PFUnDA	SDBS	DiBP
High	2	2	10	20
Median	0.2	0.2	1	2
Low	0.02	0.02	0.1	0.2

(mg/kg)

Table S2. Suspicious pollutants with significant regional differences (p<0.05) detected in the blood samples of crucian carps captured in north bays (MLB and ZSB) versus south bay (HZ) of Taihu lake.

Fraction	m/z	Retention time (min)	Accepted Compound ID	Formula	Name	Category	p-MLB/HZ	p-ZSB/HZ	HZ mean	MLB mean	ZSB mean
F1-NEG	518.9682	6.05	CSID69649	$C_{11}HF_{21}O_2$	Perfluoroundecanoic acid	Perfluorinated substance	0.008	0	307.41	226.19	97.13
F1-NEG	498.932	5.78	CSID67068	$C_8HF_{17}O_3S$	Perfluorooctanesulfonic acid	Perfluorinated substance	0.438	0.049	1156.3	1332.68	779.71
F1-NEG	325.1836	6.12	CSID23761	$C_{18}H_{30}O_3S$	2-Dodecylbenzenesulfonic acid	Linear alkylbenzene sulfonate	0.362	0.493	696.18	638.81	820.46
F1-POS	580.3522	10.25	CSID4445369	$C_{32}H_{42}N_4O_5$	Carpipramine maleate	Pharmaceutical	0.001	0	347.81	213.77	163.07
F1-POS	618.115	6.92	CSID391993	$C_{27}H_{29}ClNO_{11}$	Doxorubicin hydrochloride	Pharmaceutical	0.091	0	859.64	1266.07	1819.02
F1-POS	650.1144	5.37	CSID30791032	$C_{16}H_{34}N_7NaO_{14}S_8$	Sodium (6R,7S)-7-({[(2-amino-2-carboxyethyl)sulfanyl]acetyl}amino)-7-methoxy-3-{[(1-methyl-1H-tetrazol-5-yl)sulfanyl]methyl}-8-oxo-5-thia-1-azabicyclo[4.2.0]oct-2-ene-2-carboxylate hydrate (1:1:7)	Pharmaceutical	0.092	0.003	202.76	323.23	455.34
F1-POS	616.1362	9.52	CSID4514929	$C_{22}H_{27}N_9O_7S_2$	cefteram pivoxil	Pharmaceutical	0.229	0	35559.06	46759.06	84273.01
F1-POS	664.1611	5.72	CSID90280	$C_{29}H_{30}F_3NO_{12}$	N-Trifluoroacetyladriamycinol	Pharmaceutical	0.477	0.029	145.09	194.48	332.39
F1-POS	617.1741	9.66	CSID4444501	$C_{34}H_{30}N_2O_6S$	Pyrantel pamoate	Pharmaceutical	0.631	0.016	4609.38	5221.16	8976.69
F2-NEG	588.4165	5.29	CSID390053	$C_{32}H_{53}N_2O_4^+$	Rocuronium	Pharmaceutical	0.001	0	620.04	362.47	343.09
F2-NEG	826.4012	5.69	CSID389123	$C_{35}H_{62}NO_{15}P$	Oleandomycin 2'-O-phosphate	Pharmaceutical	0.001	0.001	139.56	244.44	261.75
F2-NEG	597.4584	4.35	CSID45603	$C_{26}H_{54}N_{10}O_2$	Ipexidine	Pharmaceutical	0.009	0	156.48	82.39	54.29

F2-NEG	764.4094	5.48	CSID21258204	$C_{42}H_{59}N_3O_{10}$	Cethromycin	Pharmaceutical	0.017	0.01	118.31	152.51	152.77
F2-NEG	438.3653	4.1	CSID2289328	$C_{21}H_{45}N_9O$	2,4,6-Tris(((2-((2-aminoethyl)amino)ethyl) amino)methyl)phenol	Benzene derivative	0.002	0.065	194.45	394.3	294.6
F2-POS	904.567	6.83	CSID144791	$C_{37}H_{70}N_{14}O_{11}$	Streptothricin C	Pharmaceutical	0.009	0.003	343.03	620.1	699.76
F2-POS	764.6556	7.52	CSID2317707	$C_{14}H_6I_4N_2O_2$	2-Anilino-4,5,6,7-tetraiodo-1H-isoindole-1 ,3(2H)-dione	Benzene derivative	0.014	0	1129.98	712.95	594.28
F2-POS	536.4063	6.43	CSID26036	$C_{35}H_{53}NO_3$	(±)-α-tocopherol nicotinate	Pharmaceutical	0.017	0.001	7102.11	3515.28	2451.39
F2-POS	552.2808	6.17	CSID30791401	$C_{30}H_{35}N_9O_3$	2-Hydroxy-N,N,N-trimethylethanaminium 5-(3'-{(E)-[1-(3,4-dimethylphenyl)-3-meth yl-5-oxo-4,5-dihydro-1H-pyrazol-4-yl]diaz enyl}-2'-hydroxy-3-biphenylyl)tetrazol-1-i de	Pharmaceutical	0.019	0.008	260.05	105.31	88.48
F2-POS	120.0808	1.13	CSID11008	$C_8H_{11}NO$	m-tyramine	Benzene derivative	0.021	0.002	170.77	291.96	322.79
F2-POS	397.2963	7.61	CSID4445340	$C_{23}H_{40}O_5$	Pimilprost	Pharmaceutical	0.023	0	762.82	385.08	209.44
F2-POS	550.2848	6.18	CSID10128124	$C_{21}H_{41}N_7O_{11}$	Desoxymycin	Pharmaceutical	0.03	0.013	443.26	211.95	186.07
F2-POS	552.4017	6.38	CSID4591452	$C_{30}H_{53}N_3O_6$	Aliskiren	Pharmaceutical	0.035	0.002	16799.29	10013.48	7206.56
F2-POS	580.3619	6.03	CSID2302085	$C_{31}H_{42}N_6O_4$	Tandutinib	Pharmaceutical	0.006	0.301	3252.46	1900.2	2615.99
F2-POS	723.5427	6.83	CSID8298513	$C_{49}H_{70}O_4$	2,3-Dimethoxy-5-methyl-6-[(2E,6E,10E,1 4E,18E,22E,26E,30E,34E,38E)-2,6,10,14, 18,22,26,30,34,38-tetracontadecaen-1-yl]- 1,4-benzoquinone	Benzene derivative	0.174	0.003	424.92	365.39	293.44
F2-POS	445.3663	6.67	CSID21377946	$C_{29}H_{50}O_4$	Methyl 2-hydroxy-6-icosyl-4-methoxybenzoate	Benzene derivative	0.182	0	2816.1	2405.5	1493.48
F2-POS	279.1606	5.45	CSID6524	$C_{16}H_{22}O_4$	Di-isobutyl phthalate	Plasticizer	0.843	0.049	191.5	183.0	219.2

F2-POS	784.546	6.58	CSID30791802	$C_{38}H_{74}N_2O_{13}$	(2R,3S,4R,5R,8R,10R,11R,13S,14R)-2-Ethyl-3,4,10-trihydroxy-3,5,6,8,10,12,14-heptamethyl-15-oxo-11-{[3,4,6-trideoxy-3-(dimethylamino)-β-D-xylo-hexopyranosyl]oxy}-1-oxa-6-azacyclopentadecan-13-yl 2,6-dideoxy-3-C-methyl-3-O-methyl-α-L-ribo-hexopyranoside hydrate (1:1)	Pharmaceutical	0.481	0.007	1594.55	1700.61	2189.63
F2-POS	914.5571	6.72	CSID10482078	$C_{51}H_{79}NO_{13}$	Sirolimus	Pharmaceutical	0.496	0.03	739.35	868.86	1203.49

Table S3. Parameters of the algorithms in Gephi 0.9.1 applied for network correlation analysis.

Modulation-Community Detection	
Resolution	1.0
Weights of Edges	Used
OpenOrd	
Edge Cut	0.8
Num Threads	3
Num Iterations	750
Fixed Time	0.2
Force Atlas	
Inertial	0.1
Intensity of Repulsion	200
Intensity of Gravitation	10.0
Max Displacement	10.0
Auto Stabilization	Used
Sensitivity of Auto Stabilization	0.2
Gravity	30.0
Speed	1.0
Noverlap	
Speed	3.0
Ratio	1.2
Margin	5.0

Figure S1. Sampling sites of the wild crucian carp captured in Taihu lake.

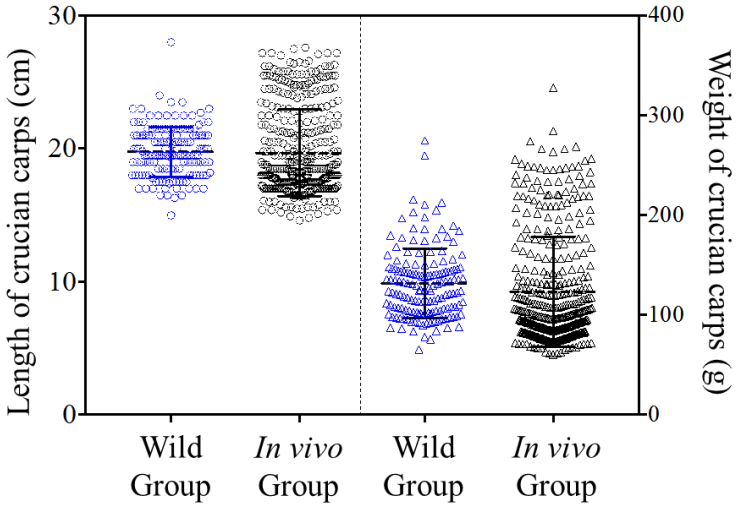

Figure S2. Body length (cm) and body weight (g) of the crucian carp captured in Taihu Lake and used in the *in vivo* exposure test.

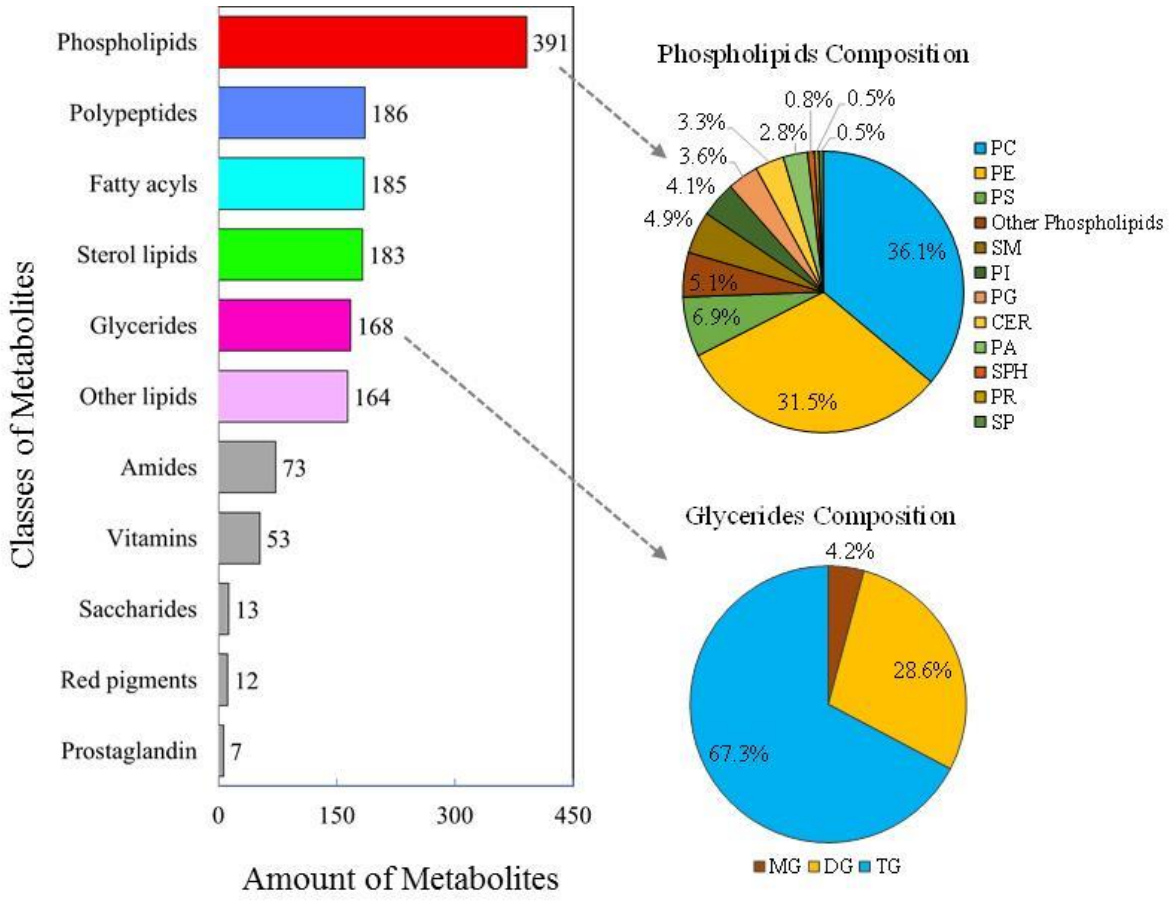

Figure S3. Percentages and numbers of the intrinsic metabolites identified in the blood of the wild carp from Taihu Lake.

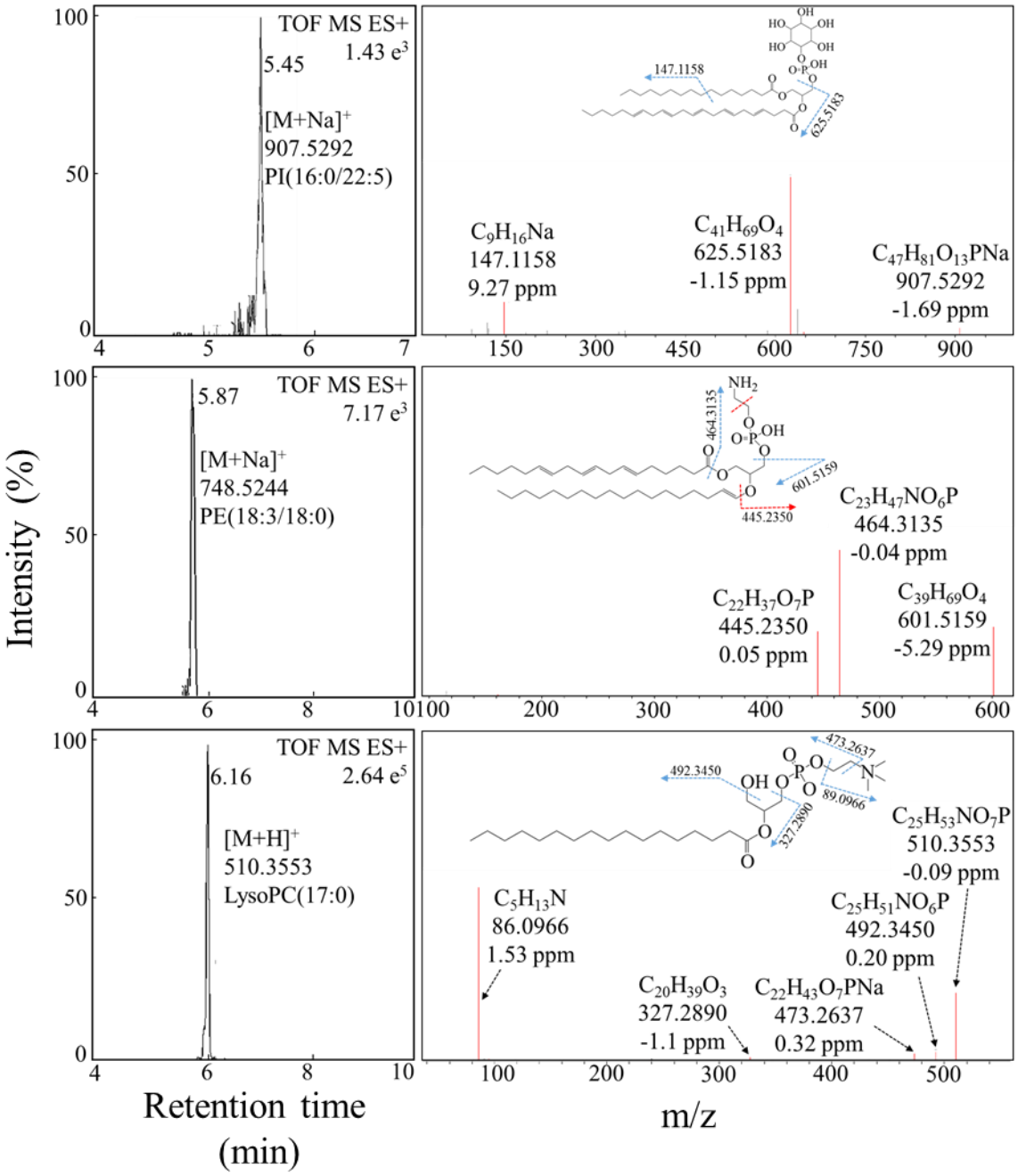

Figure S4. The chromatograms and fragmentation spectrums of phospholipids (PLs) identified in blood samples of wild crucian carp from Taihu Lake.

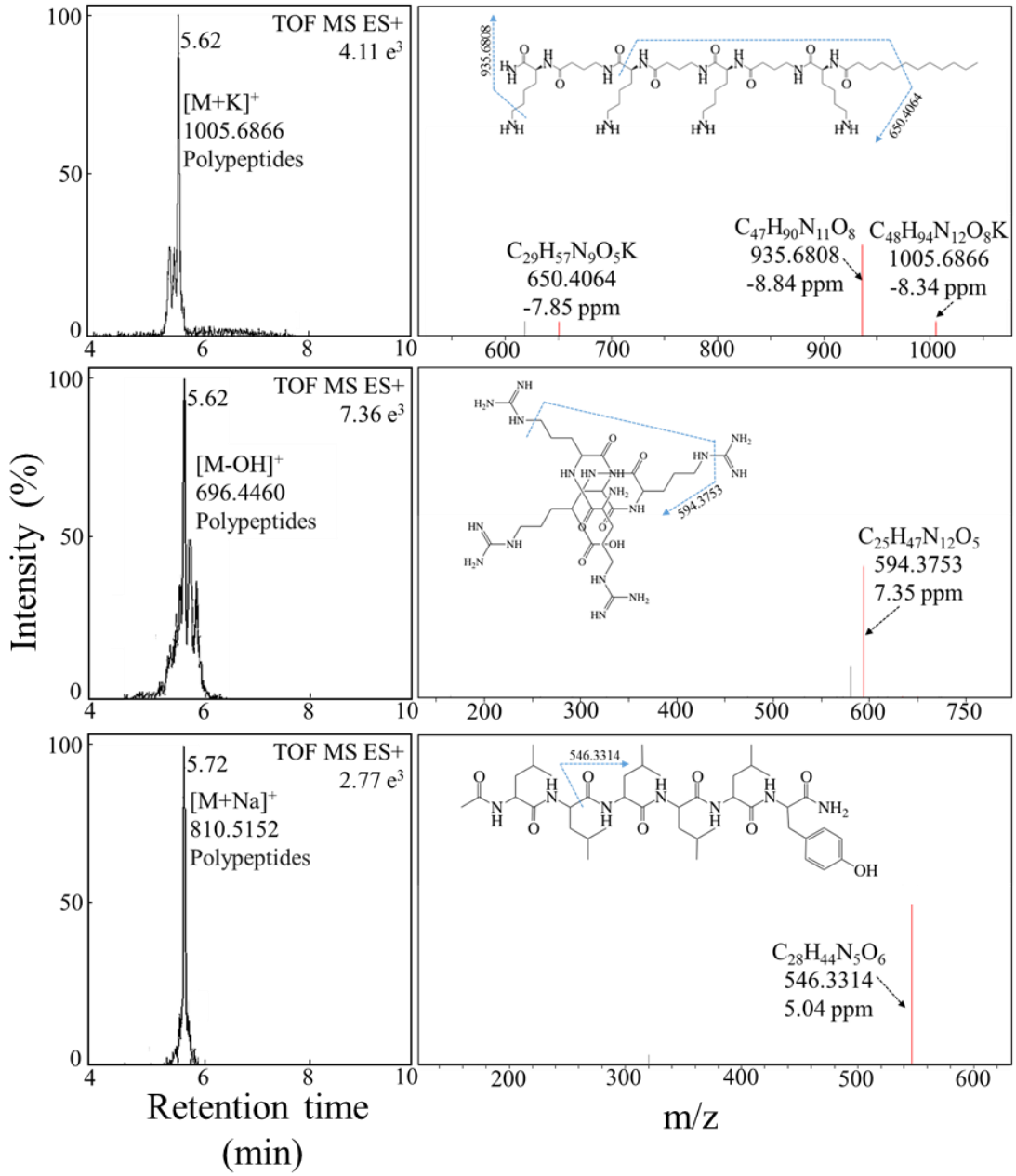

Figure S5. The chromatograms and fragmentation spectrums of polypeptides (PPs) identified in blood samples of wild crucian carp from Taihu Lake.

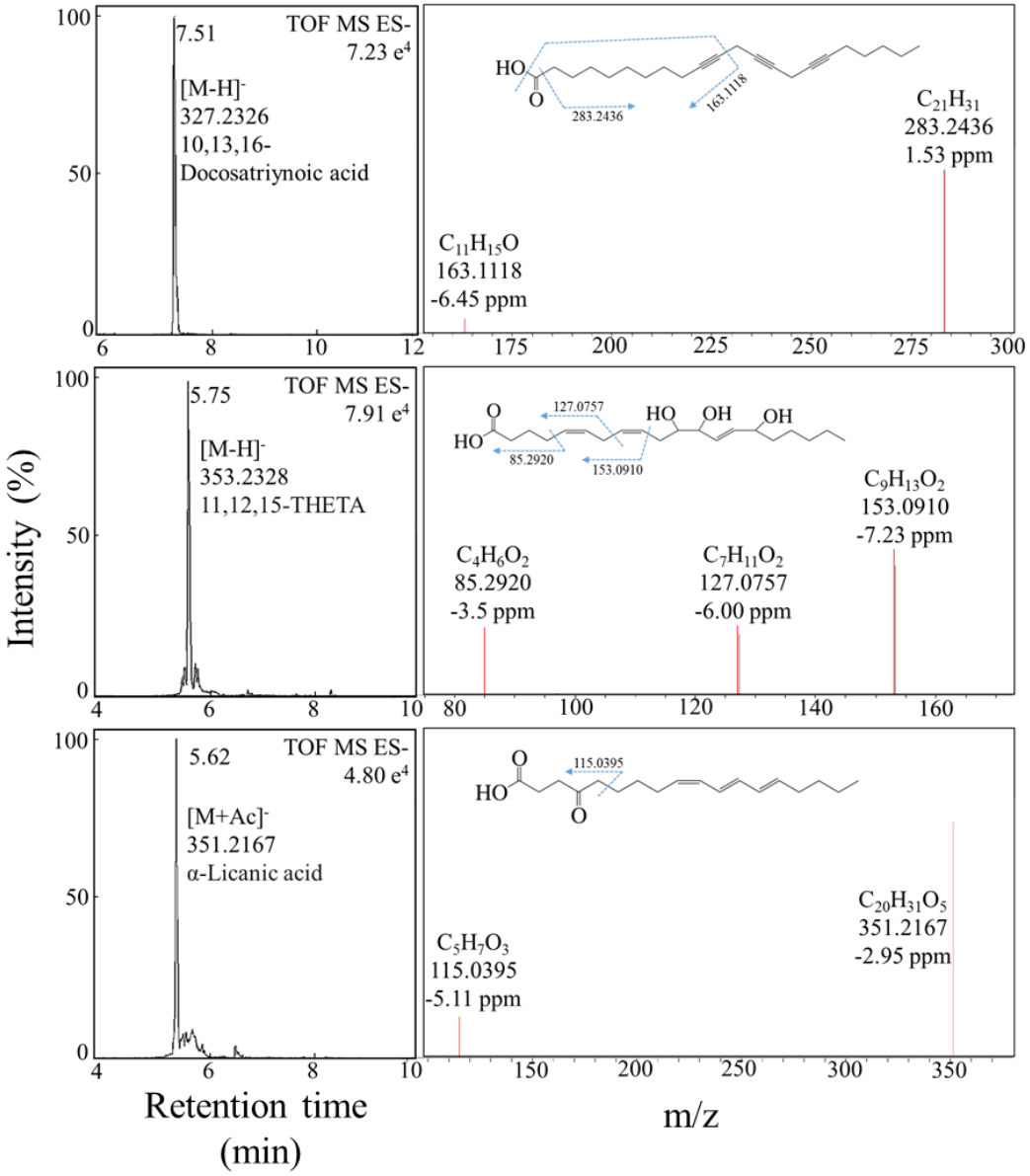

Figure S6. The chromatograms and fragmentation spectrums of fatty acyls (FAs) identified in blood samples of wild crucian carp from Taihu Lake.

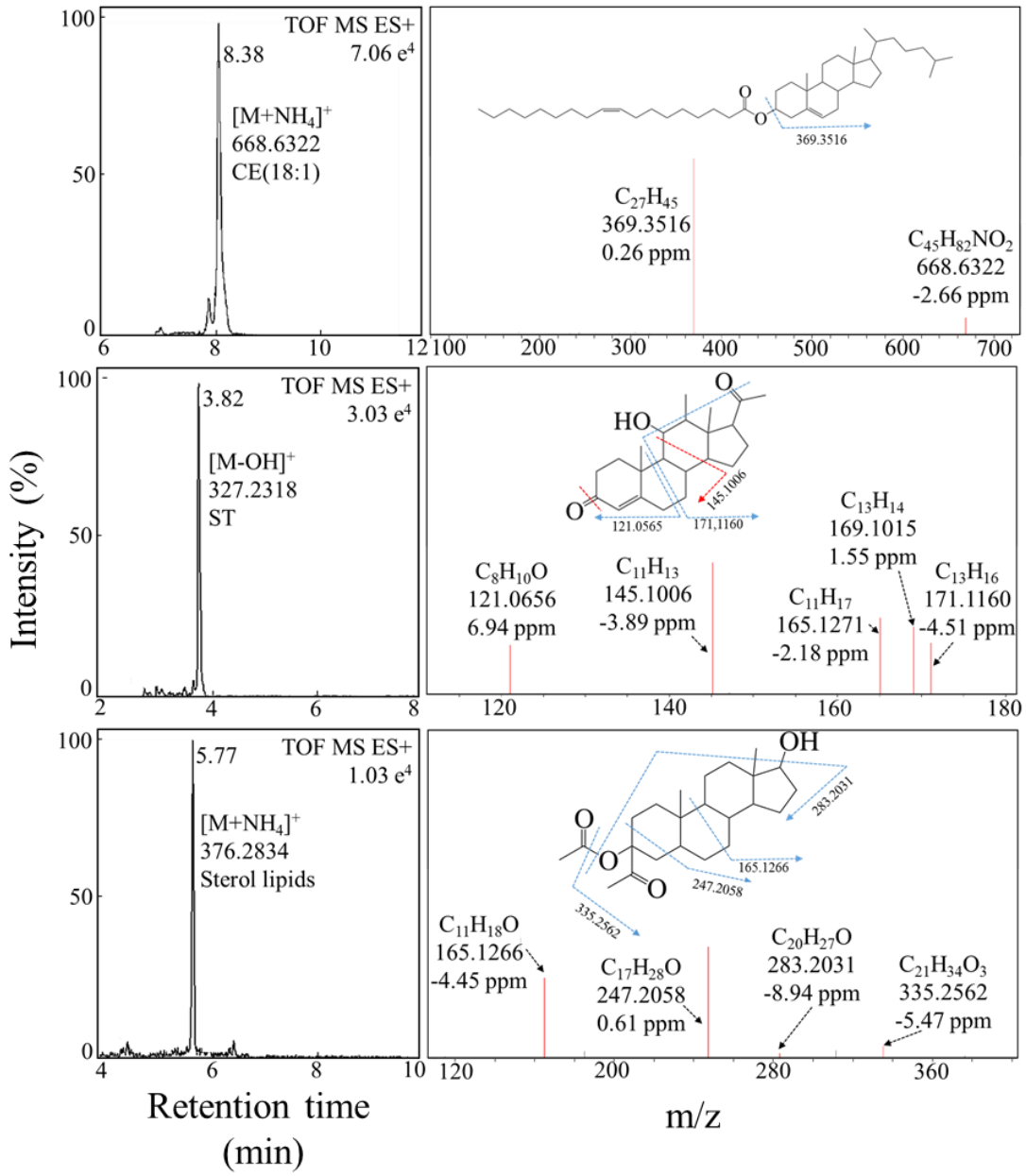

Figure S7. The chromatograms and fragmentation spectrums of sterol lipids (SLs) identified in blood samples of wild crucian carp from Taihu Lake.

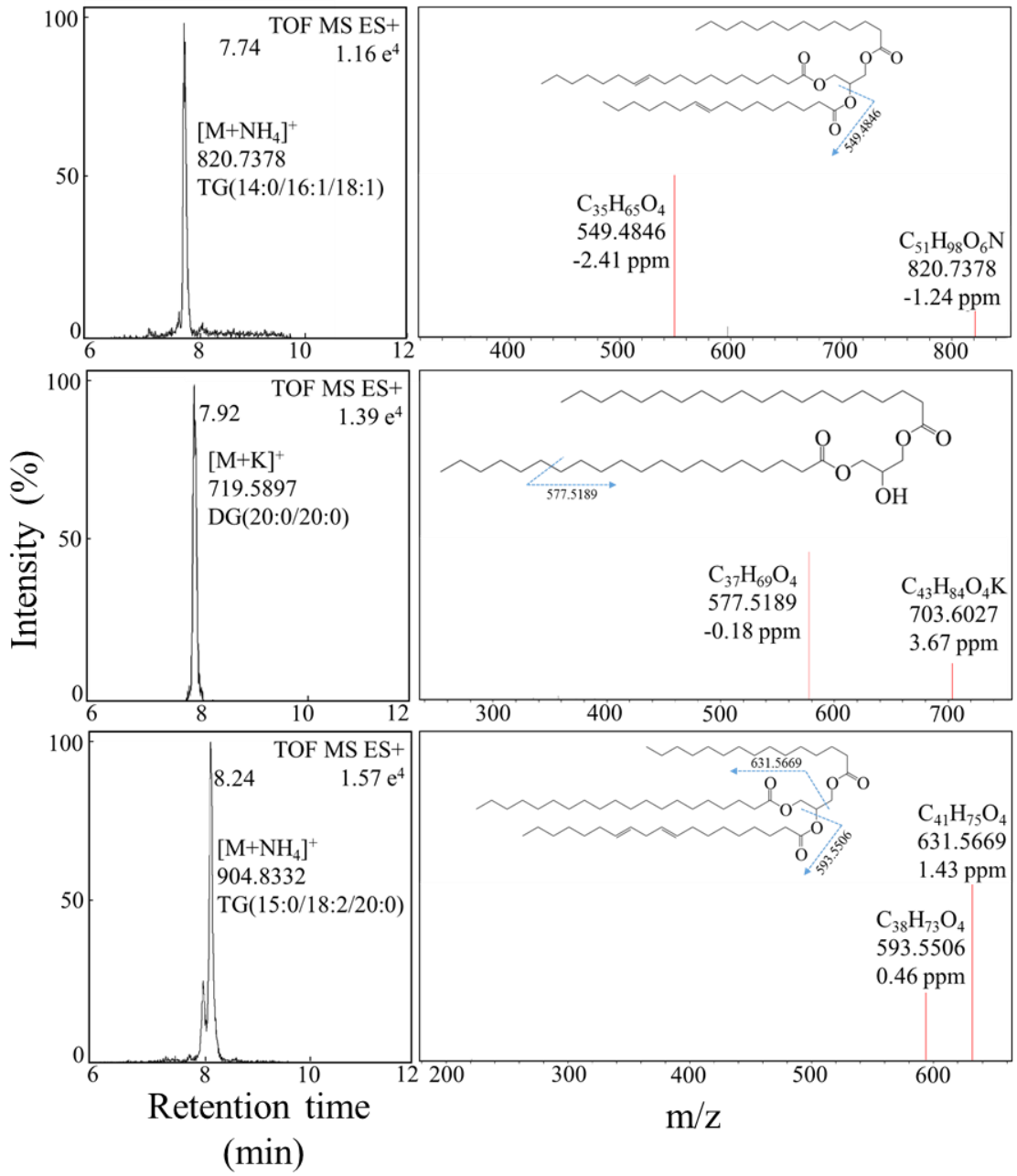

Figure S8. The chromatograms and fragmentation spectrums of glycerides (GLs) identified in blood samples of wild crucian carp from Taihu Lake.

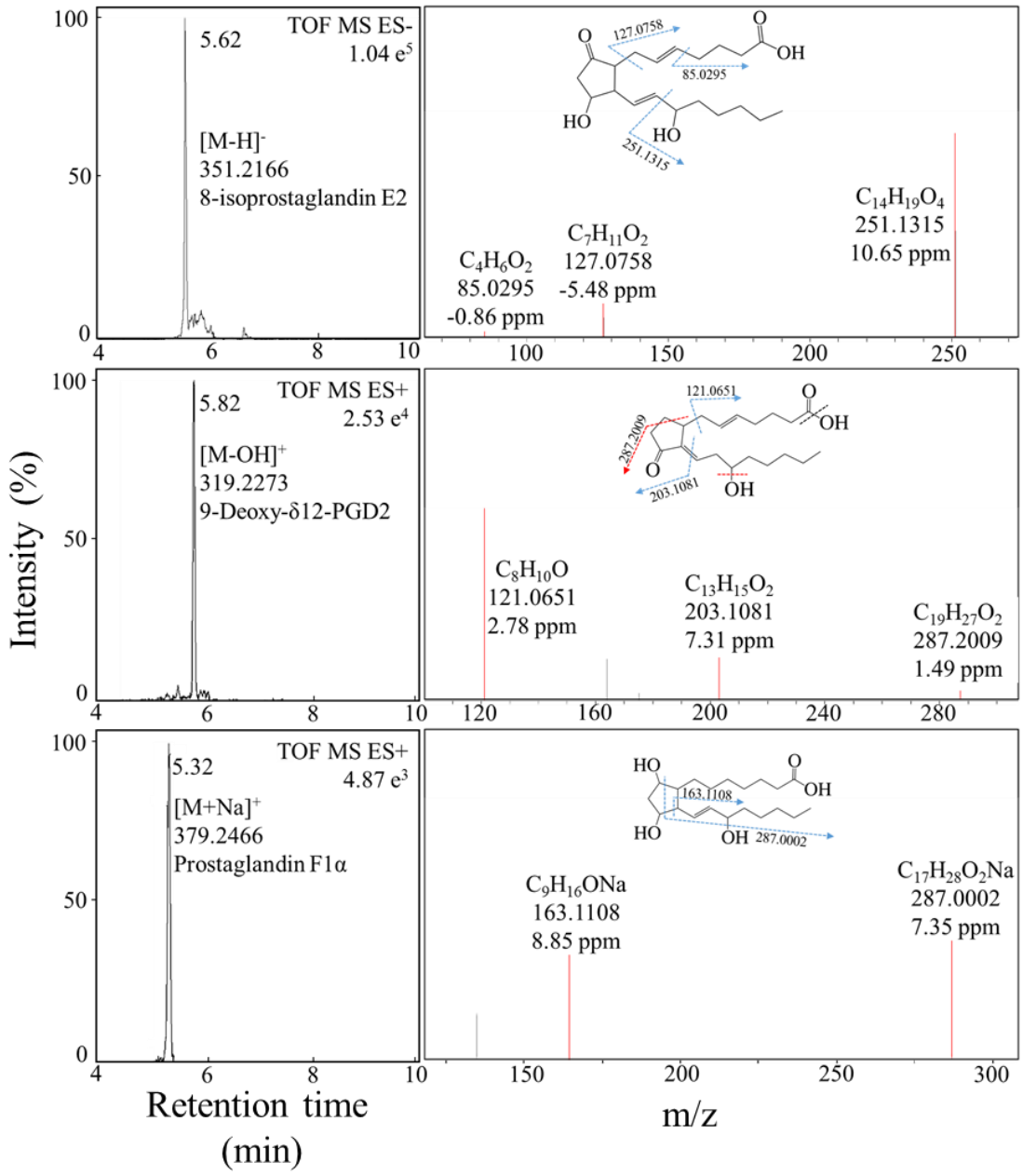

Figure S9. The chromatograms and fragmentation spectrums of prostaglandins identified in blood samples of wild crucian carp from Taihu Lake.

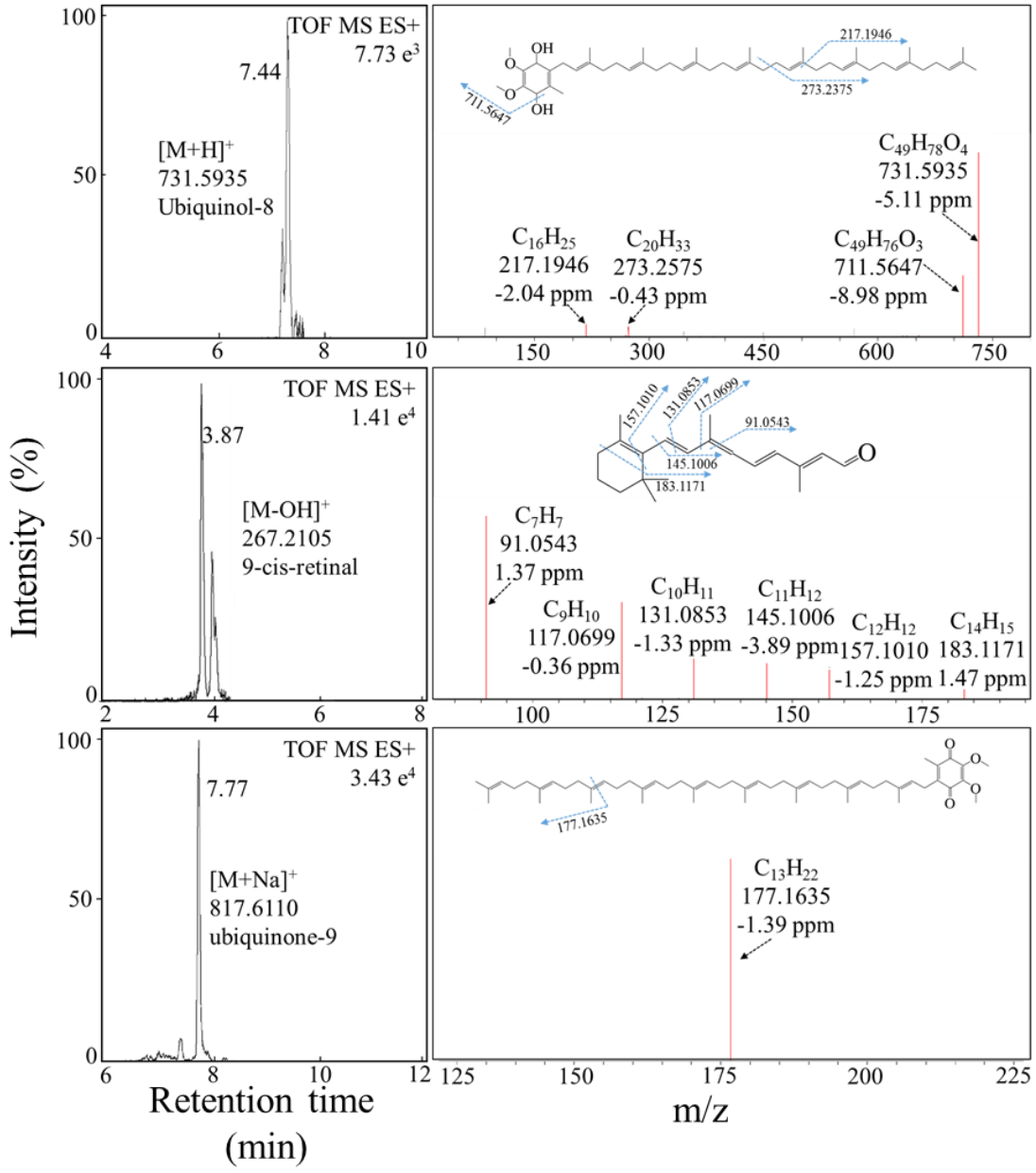

Figure S10. The chromatograms and fragmentation spectrums of vitamins identified in blood samples of wild crucian carp from Taihu Lake.

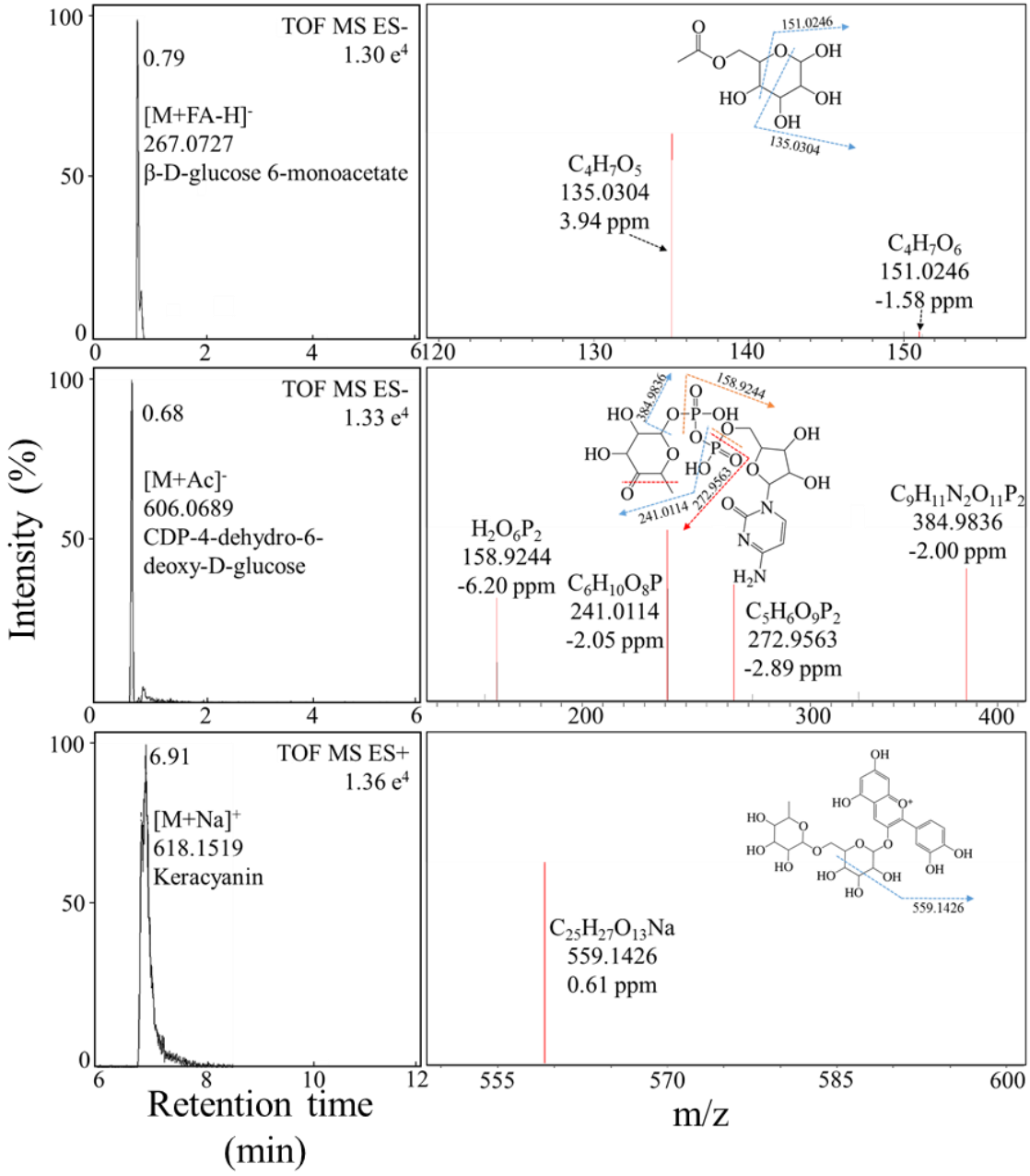

Figure S11. The chromatograms and fragmentation spectrums of saccharides identified in blood samples of wild crucian carp from Taihu Lake.

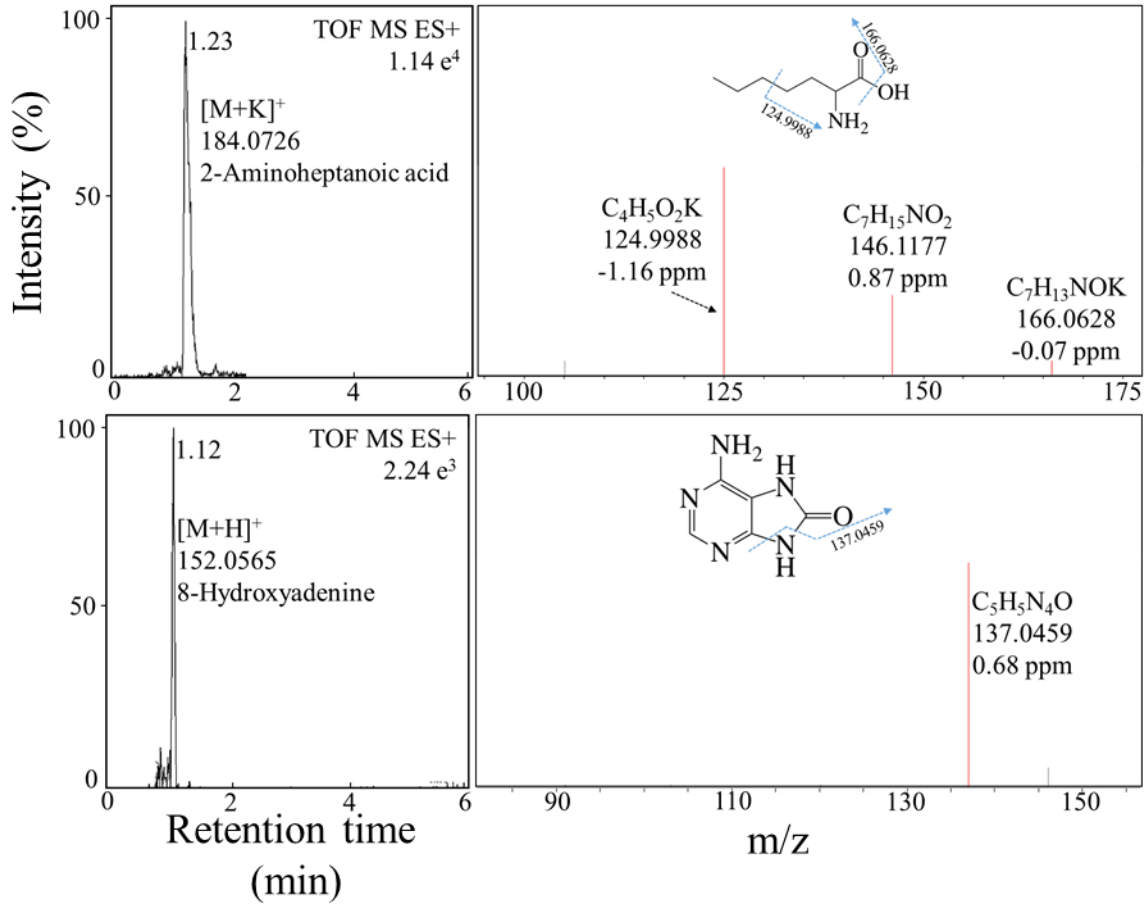

Figure S12. The chromatograms and fragmentation spectrums of amides identified in blood samples of wild crucian carp from Taihu Lake.

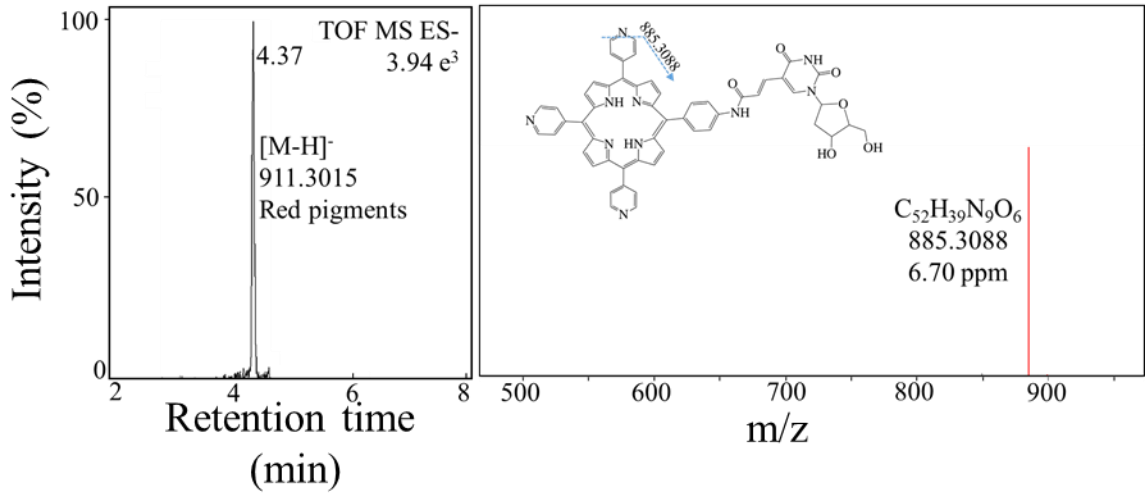

Figure S13. The chromatograms and fragmentation spectrums of red pigments identified in blood samples of wild crucian carp from Taihu Lake.

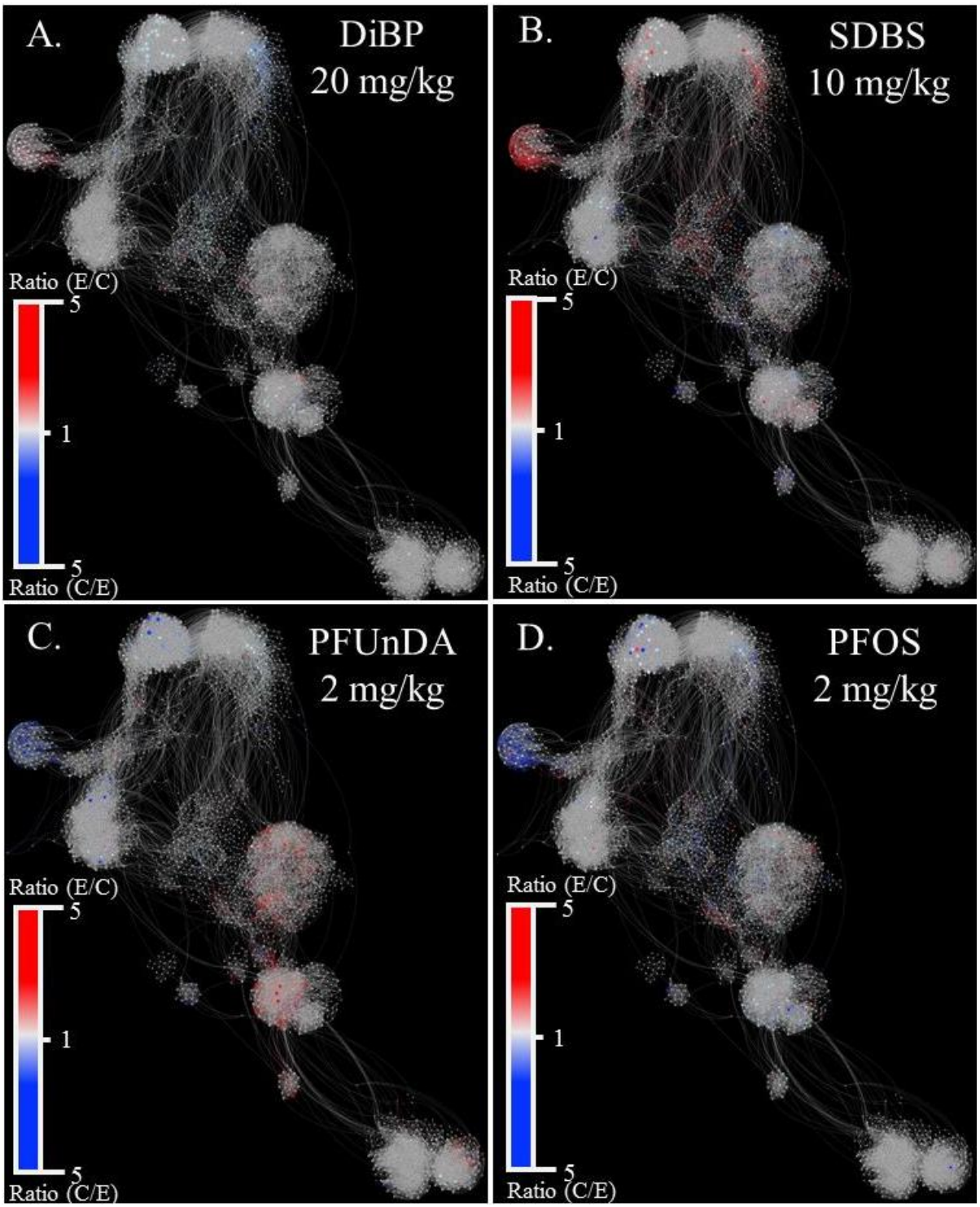

Figure S14. Profile variations of the intrinsic metabolites in carp exposed to the identified exogenous pollutants (*in vivo*). (A). DiBP, (B). SDBS, (C). PFUnDA, (D). n-PFOS.

References

1. Braga, C. P.; Boone, C. H.; Grove, R. A.; Adamcova, D.; Fernandes, A. A. H.; Adamec, J.; de Magalhães Padilha, P. Liver proteome in diabetes type 1 rat model: Insulin-dependent and-independent changes. *OMICS: J Integrative Biol*. **2016**, *20*, 711-726.
2. Gao, S.; Wan, Y.; Li, W.; Huang, C. Visualized Networking of Co-Regulated Lipids in Human Blood Based on High-Throughput Screening Data: Implications for Exposure Assessment. *Environ Sci Technol*. **2019**, *53*, 2862-2872.
3. Sumner, L. W.; Amberg, A.; Barrett, D.; Beale, M. H.; Beger, R.; Daykin, C. A.; Fan, T.; Fiehn, O.; Goodacre, R.; Griffin, J. L. Proposed minimum reporting standards for chemical analysis. chemical analysis working group (CAWG) metabolomics standards initiative (MSI). *Metabolomics*. **2007**, *3*, 211-221.
4. Pietiläinen, K. H.; Sysi-Aho, M.; Rissanen, A.; Seppänen-Laakso, T.; Yki-Järvinen, H.; Kaprio, J.; Orešič, M. Acquired obesity is associated with changes in the serum lipidomic profile independent of genetic effects–a monozygotic twin study. *PloS one*. **2007**, *2*, e218.
5. Steuer, R. Review: on the analysis and interpretation of correlations in metabolomic data. *Brief Bioinform*. **2006**, *7*, 151-158.